ELSEVIER

Biochimica et Biophysica Acta 1365 (1998) 435–442

BIOCHIMICA ET BIOPHYSICA ACTA
BBA

Stopped-flow kinetic studies of low potential electron carriers of the photosynthetic bacterium, *Rhodobacter capsulatus*: ferredoxin I and NifF

Patrick C. Hallenbeck *, Giuseppa Gennaro

Département de Microbiologie et Immunologie, Université de Montréal, C.P. 6128, Succursale Centre-Ville, Montreal, Que. H3C 3J7, Canada

Received 2 February 1998; revised 27 March 1998; accepted 2 April 1998

Abstract

The kinetics of electron-transfer reactions involving *nif*-specific proteins from *Rhodobacter capsulatus*; ferredoxin I, NifF, Fe-protein of nitrogenase and dithionite were studied using stopped-flow spectrophotometry. Kinetic evidence was obtained for the formation of a tight (0.44 μM) complex between NifF and Fe-protein. Under the same conditions, FdI interacted only weakly ($K_d > 325$ μM) with Fe-protein. There was no evidence for complex formation between NifF and FdI since the reaction $NifF_{SQ}+FdI_{red}$ had a bimolecular rate constant of $12.5 \pm 1.2 \times 10^3$ M^{-1} s^{-1}. These results suggest that NifF, which is present in only small quantities in the cell, can make a significant contribution to the overall rate of nitrogen fixation due its high reactivity with Fe-protein. Moreover, the apparent lack of specific interaction between NifF and FdI suggest that they act in vivo in parallel to reduce Fe-protein and not in series.

Keywords: Nitrogenase; Ferredoxin I; *nif*-specific Flavodoxin; Stopped-flow kinetics; (*Rhodobacter capsulatus*)

1. Introduction

Flavodoxins are low molecular weight proteins containing FMN that act as low-potential electron carriers in a variety of systems. A great deal is presently known about the structure and function of flavodoxins (for a recent review see [1]). Of particular interest to the investigation reported here, a large number of studies have examined the factors controlling the electron transfer capabilities of flavodoxins. However, most of these studies have described the interaction of flavodoxin with non-physiological redox partners, such as high-potential iron protein (HiPIP) [2] and cytochrome *c* [3–10].

In some cases, flavodoxin is induced under conditions of iron limitation where it serves as a replacement for ferredoxin in various aspects of cellular metabolism, e.g. photosynthesis. In other cases, flavodoxin is induced as part of a specific metabolic pathway. For example, in *Klebsiella pneumoniae* (Kp), a *nif*-specific flavodoxin, NifF, forms a specific electron transport pathway from NifJ (pyruvate: flavodoxin oxidoreductase) to the Fe-protein component of nitrogenase. In this case, NifF appears to be the sole electron carrier to nitrogenase in vivo since *nifF* mutants are Nif^-. The interaction of Kp NifF with nitrogenase has been studied using

Abbreviations: FdI, ferredoxin I; FdII, ferredoxin II; NifF, the *nif*-specific flavodoxin; X_{red}, reduced electron carrier; X_{ox}, oxidized electron carrier; HQ, hydroquinone; SQ, semiquinone; IPTG, isopropylthiogalactoside; FMN, flavin mononucleotide

* Corresponding author. Fax: +1 (514) 343-5701; E-mail: hallenbe@ere.umontreal.ca

0005-2728/98/$19.00
PII: S0005-2728(98)00096-6

stopped-flow spectrophotometry [11], and it was demonstrated that NifF and Fe-protein (complexed with MgATP) form a tight complex ($K_d = 13$ μM). This system exhibits exquisite specificity since a highly similar flavodoxin, NifF from *Azotobacter chroococcum*, interacts only very weakly with Kp Fe-protein ($K_d \geq 1000$ μM). However, at present the molecular basis for this specificity is unknown. In addition, it has not been established until now if homologous systems present the same degree of specificity.

Electron transfer pathways to nitrogenase in other organisms are much less clear. The results of in vitro analyses of the capacity to drive nitrogenase activity in a coupled system have been used to suggest possible in vivo electron carriers to nitrogenase. However, the ability to extrapolate the results of these relatively non-specific assays to the in vivo system has yet to be demonstrated and is therefore questionable. Genetic studies, for the organisms where this has been carried out, have produced equivocal results that are difficult to interpret. An electron transport chain to nitrogenase in *Azotobacter* consisting of FdI and flavodoxin was suggested based on their ability to couple the reducing power generated by illuminated chloroplast fragments to nitrogenase [12]. However, genetic studies have shown that neither FdI nor NifF are absolutely required for nitrogen fixation by *Azotobacter vinelandii* [13].

The photosynthetic bacterium *Rhodobacter capsulatus* has been shown to contain a plethora of low-potential electron carriers [14–24]. However, relatively little is known about their physiological function; including how these carriers are reduced and the identity of their in vivo electron acceptor. Four ferredoxins; FdI, FdIII, FdIV and FdV, and flavodoxin (NifF), are encoded by *nif*-specific genes and therefore presumably play some role in nitrogen fixation. However, in vitro studies have shown that of these only FdI and NifF can potentially donate electrons to the Fe-protein component of nitrogenase in vivo. Genetic studies have failed to clarify this question. FdI mutants are practically Nif^-; however, the interruption of the FdI gene causes pleiotropic effects, including decreased stability of the nitrogenase proteins [25] and decreased transcription of the NifF gene (unpublished results). NifF mutants retain their ability to fix nitrogen, albeit at a reduced (59%) rate [24]. In an attempt to understand this complex situation, we have initiated the study of the kinetics and possible physical interactions involved in electron transfer and complex formation between the various potentially competent electron carriers of *R. capsulatus* and the Fe-protein component of nitrogenase.

2. Materials and methods

2.1. Purification and manipulation of proteins

FdI [14], FdII [15] and the Fe-protein component of nitrogenase [26] were purified essentially as previously described. In order to obtain sufficient quantities of NifF for these studies, we developed a scheme to overexpress NifF from *R. capsulatus* in *Escherichia coli* and purify the recombinant protein. As a first step, *nifF* containing convenient flanking restriction sites was obtained by PCR amplification using a 3.2-kb *Pst*I DNA *nifF*-containing fragment from pGR1-1 [24] as template and GC127 (5′-ATTCCTG-ACAATTTTGCCCG-3′) plus GN835 (5′-GGTCT-TTCATGGGCAGGTCT-3′) as primers. PCR (10 μl of each of the phosphorylated primers (GC127 and GN835), 16 μl of dNTP stock pool at 1.25 mM, 20 ng of template DNA, 2.5 U of *Taq* DNA polymerase (Gibco BRL) covered with 40 μl oil (modified from [27]) was carried out for 25 cycles with 1-min steps at 94 and 57°C, and primer extension at 72°C for 2 min. A 708-bp fragment obtained was used for the construction of pGGR3 using *Eam*11051 digested BSII TKS(−) [28] for the direct cloning of PCR products. To construct a plasmid capable of the IPTG-inducible overexpression of *nifF*, a *Sma*I and *Sal*I fragment from pGGR3 was cloned within the same sites in p*Trc*99A (Pharmacia Biotech), yielding pGGR4, which was introduced into *E. coli* DH10B by electrotransformation [29].

For production of *R. capsulatus* NifF protein, *E. coli* DH10B/pGGR4, grown overnight aerobically in LB ampicillin, was used to inoculate 20 l of Terrific Broth media. IPTG (0.5 g/20 l) was added when a cell density of about 0.6 at A_{600} had been obtained, and the culture was incubated aerobically for an additional 10 h at 37°C. Bacteria were harvested by centrifugation using a Sharples centrifuge and stored

at −20°C. NifF purification was carried out aerobically. Cells (~500 g wet weight) were thawed in 500 ml of 0.1 M Tris-HCl buffer (pH 7.4) and sonicated at 4°C five to seven times (1 min) at maximal power with a Biosonick III. The sonicate was clarified by centrifugation (16 300 g, 3 h) at 4°C. The crude extract was loaded on a DEAE-cellulose column (DE52; 8×2.5 cm) previously equilibrated with 50 mM Tris-HCl buffer (pH 7.4; hereafter referred to as buffer). The column was then eluted stepwise: 100 mM NaCl in buffer; 160 mM NaCl in buffer; 260 mM NaCl in buffer. The 260 mM NaCl step eluted recombinant flavodoxin as a green coloured fraction, which turned yellow upon storage at −20°C. This fraction was further concentrated on a small DE52 column and desalted on a Sephadex G-50 column. Final purification to homogeneity ($A_{274}/A_{450} = 0.233$) was achieved by FPLC using a Hi-Load 26/10 Q-sepharose high-performance anion exchange column (Pharmacia Biotech) and the previously described elution conditions for NifF from *K. pneumoniae* [30]. The final yield was 88 mg.

All other manipulations, except where specifically noted, were carried out under strictly anaerobic conditions, either in an anaerobic chamber or using lines carrying nitrogen that had been passed through a heated tower of BASF catalyst. Fully reduced species (FdI_{red}, $FdII_{red}$, $NifF_{HQ}$) were generated by the addition of a small excess of sodium dithionite which was subsequently removed by gel filtration through a small column of PDG 8 (equilibrated and eluted with 25 mM HEPES 10 mM $MgCl_2$ (pH 7.4)) in the anaerobic chamber. The oxidized species were exchanged into 25 mM HEPES 10 mM $MgCl_2$ (pH 7.4) where necessary using the same technique. $NifF_{SQ}$ was conveniently generated by mixing equimolar amounts of anaerobically prepared, dithionite-free, $NifF_{ox}$ and $NifF_{HQ}$.

2.2. Mid-point potential determinations

Oxidation-reduction potentials were determined spectrophotometrically at 25°C in 50 mM HEPES buffer, pH 7.4. The potential of the NifF OX/SQ couple was determined by exposing an approximately equimolar solution of NifF and indigo-5,5′-disulphonate ($E_{m7} = -125$ mV (SHE)), which also contained 30 mM EDTA, to visible light for short intervals of time. The extent of flavodoxin reduction was determined at 458 nm (an isobestic point between the oxidized and reduced forms of indigo-5,5′-disulphonate). The extent of dye reduction was calculated from the absorbance at 608 nm after correction for the contribution of the semiquinone form of flavodoxin. The determined equilibrium constant was used in conjunction with the Nernst equation to calculate the mid-point potential using least squares linear regression analysis.

The potential of the NifF SQ/HQ couple was determined by complete reduction of NifF to the hydroquinone form with excess sodium dithionite followed by subsequent titration to the semiquinone state with sodium sulphite. The obtained redox potentials were ascertained in parallel experiments using methyl viologen ($E_{m7} = -446$ mV (SHE)). The mid-point potential of flavodoxin was calculated using the Nernst equation and the determined experimental redox potential and the relative concentrations of the semiquinone and hydroquinone forms of flavodoxin.

2.3. Kinetic analysis

All kinetic experiments were carried out at 25 ± 0.1°C in 25 mM HEPES, 10 mM $MgCl_2$, pH 7.4. Transient kinetics were monitored with a stopped-flow spectrophotometer (model SF-61), Hi-Tech Scientific, installed in an anaerobic glove box ($O_2 < 1$ ppm). Data were recorded through an RS232 interface with a microcomputer and analysed using the KinetAssyt Program, Hi-Tech Scientific, with fitting by non-linear least-squares analysis to a single exponential. All experiments fit well to a single ex-

Table 1
Redox potentials of FdI, FdII, and NifF from *R. capsulatus*

Protein	Mid-point potential	Reference
FdI	−490 mV[a]	[32]
	−510 mV[b]	[33]
FdII	−430 mV (3Fe-4S)[b]	
	−630 mV (4Fe-4S)[b]	[34]
NifF	−158 ± 2 mV (Ox/SQ)[c]	
	−474 ± 5 mV (SQ/HQ)[c]	This study

[a]EPR titration.
[b]Cyclic voltammetry.
[c]Spectrophotometric titration.

ponential function. Each point represents the average of at least four independent traces.

3. Results and discussion

3.1. Redox properties of FdI, FdII and NifF

The mid-point redox potentials of FdI and FdII have been previously determined (Table 1). FdI, which has two 4Fe-4S clusters, demonstrates a single mid-point potential of −490 mV (EPR titration) or −510 mV (cyclic voltammetry). FdII, which is analogous to the well-characterized FdI of *A. vinelandii*, contains a 3Fe-4S cluster with a mid-point potential of −430 mV and a 4Fe-4S cluster with a mid-point potential of −630 mV. We used spectrophotometric methods to determine the redox potentials of NifF from *R. capsulatus*. We found that the E_{m7} of the OX/SQ couple, −158 mV, was the same as the NifF from *K. pneumoniae* [31] and the E_{m7} of the SQ/HQ couple, −474 mV, was intermediate between that of *K. pneumoniae*, −422 mV [31] and *A. chroococcum*, −522 mV [31].

3.2. Reduction of FdI and FdII by dithionite

We examined the kinetics of the reduction of FdII by dithionite. As far as we are aware this is the first examination of this sort for a 4Fe-4S, 3Fe-4S ferredoxin. As expected, a linear relationship was obtained between k_{obs} and $[S_2O_4^{2-}]^{1/2}$ (Fig. 1), indicating that the $SO_2^{\bullet-}$ species is the active reductant. The bimolecular rate constant, k_2, for this reaction is 16.5 ± 1.1 $M^{-1/2}$ s^{-1} (Fig. 1). Thus the rate of reduction of FdII by dithionite is comparable to that previously observed for the 2Fe-2S ferredoxin from spinach (8.6 $M^{-1/2}$ s^{-1}) or for 2 [4Fe-4S] ferredoxins (11 $M^{-1/2}s^{-1}$, 19 $M^{-1/2}$ s^{-1}) [35]. The amplitude of the absorbance change observed was consistent with the complete reduction of both clusters of FdII, whereas the observed rates of reduction were well fit by a single exponential function indicating that the two different clusters are indistinguishable by this criteria. The appreciable intercept observed indicates a significant rate of reverse reaction (2.89 ± 0.1 s^{-1}), which is to be expected due to the extremely low potential of the 4Fe-4S cluster. On the other hand, reduction of FdI was comparatively sluggish (Fig. 2) with a bimolecular rate constant of 1.69 ± 0.14 $M^{-1/2}$ s^{-1}. In agreement with its previously determined redox potential (−490 mV, −510 mV, Table 1), there was little evidence of a reverse reaction. As $S_2O_4^{2-}$ is in rapid equilibrium with the $SO_2^{\bullet-}$ radical anion;

$$S_2O_4^{2-} \underset{k_{-1}}{\overset{k_{+1}}{\rightleftharpoons}} 2\,SO_2^{\bullet-}$$

the fact that the observed rate constant is proportional to $[S_2O_4^{2-}]^{1/2}$ indicates that the reduction of these ferredoxins occurs mainly by the $SO_2^{\bullet-}$ radical. Therefore the true rate constant, k, is related to the apparent rate constant, k_{app}, by $k = k_{app}/K_{DT}$, where $K_{DT} = k_1/k_{-1}$, =1.4 nM under the conditions used here [36]. Thus, the true rate constants for reduction of FdI and FdII are, 5.3×10^4 M^{-1} s^{-1} and 5.2×10^5 M^{-1} s^{-1}. These compare favourably with those determined for ferredoxin I and ferredoxin II form *Desulfovibrio desulfuricans*, 6×10^4 M^{-1} s^{-1} and 4×10^5 M^{-1} s^{-1} [37].

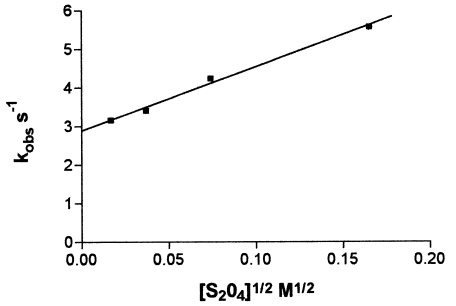

Fig. 1. Dependence of k_{obs} on dithionite concentration for the reduction of FdII by dithionite. The data were obtained by stopped-flow spectrophotometry at 395 nm with $[FdII_{ox}]$ 36 μM and $[S_2O_4^{2-}]$ varied between 0.27 and 27.3 mM.

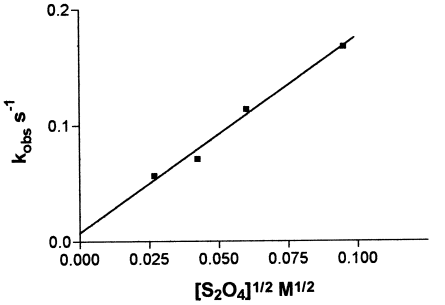

Fig. 2. Dependence of k_{obs} on dithionite concentration for the reduction of FdI by dithionite. The data were obtained by stopped-flow spectrophotometry at 395 nm with $[FdI_{ox}]$165 μM and $[S_2O_4^{2-}]$ varied between 0.72 and 9 mM.

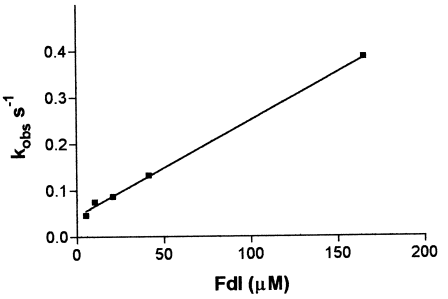

Fig. 3. Dependence of k_{obs} on FdI_{ox} concentration for the oxidation of $NifF_{HQ}$ by FdI_{ox}. The data were obtained by stopped-flow spectrophotometry at 395 nm with $[NifF_{HQ}]$ 4.4 μM and $[FdI_{ox}]$ varied between 5.2 and 165 μM.

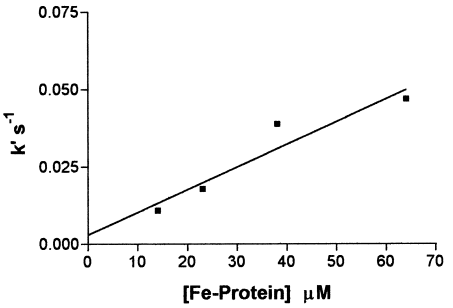

Fig. 5. Reduction of FdI_{ox} by dithionite catalyzed by Fe-protein. The data were obtained by stopped-flow spectrophotometry at 395 nm with: $[FdI_{ox}]$, 15.7 μM; dithionite, 0.85 mM; and Fe-protein varied between 14 and 64 μM. Data are plotted as k' (where $k' = k_{obs} - k_{obs}$ ([Fe-P] = 0) versus [Fe-protein].

3.3. Interaction of NifF with FdII and FdI

We examined the interaction of NifF with FdII and FdI by following the oxidation of $NifF_{HQ}$ by the oxidized ferredoxin species. In both cases, the experimental data fit well to pseudo-first-order kinetics. Plots of k_{obs} versus [Fd] were linear throughout the ranges of oxidized ferredoxin tested suggesting that there is little specificity for complex formation between NifF and the two different ferredoxins. The apparent bimolecular rate constants obtained from the slopes of plots of k_{obs} versus [Fd] were: FdI, $2.08 \pm 0.05 \times 10^3$ M^{-1} s^{-1} (Fig. 3), FdII, $24 \pm 1 \times 10^3$ M^{-1} s^{-1} (results not shown). The reverse reaction for the NifF-FdI couple was also examined. Again, the reaction gave no indication of saturation, and a plot of k_{obs} versus [Fd] was linear with an apparent bimolecular rate constant of $12.5 \pm 1.2 \times 10^3$ M^{-1} s^{-1} (Fig. 4). A lower limit to K_d can be estimated as $K \geq 2500$ μM (Table 2), if one assumes that curvature would have been observed at the highest [Fd] if it was 20% of K_d. The ratio of the forward and reverse rate constants determined here, 0.166, is in relatively good agreement with the theoretical value calculated from a consideration of the relevant redox potentials, 0.246. (The equilibrium constant was calculated according to E_{m7} (A) $- E_{m7}$ (B) = RT/nF ln$K$.) We examined the potential role of electrostatic interactions in the reaction between NifF and FdI by examining the variation in k_{obs} with ionic strength (varied by addition of NaCl up to a final concentration of 0.81 M). The linear portion of a plot of ln k_{obs} versus $[NaCl]^{1/2}$ gave a slope of -0.98 ± 0.07 (results not shown), indicating that electrostatic forces, either positive or negative, do not play a significant role in the interaction of NifF and FdI.

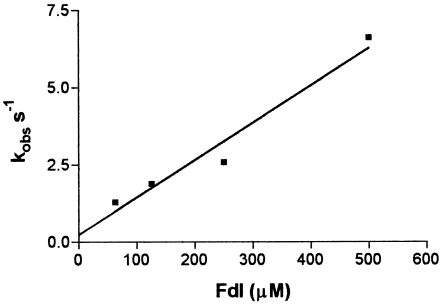

Fig. 4. Dependence of k_{obs} on FdI_{red} concentration for the reduction of $NifF_{SQ}$ by FdI_{red} The data were obtained by stopped-flow spectrophotometry at 580 nm with $[NifF_{SQ}]$ 4.0 μM and $[FdI_{red}]$ varied between 62.5 and 500 μM.

3.4. Interaction of NifF and FdI with nitrogenase Fe-protein

Of course, of major interest is the interaction of FdI and NifF with the Fe-protein of nitrogenase (all components from *R. capsulatus*) as steady-state experiments in which potential electron carriers mediate electron flow from illuminated chloroplast fragments to nitrogenase have shown that both are capable of reducing nitrogenase in this system [14,23]. In order to study the interaction of *R. capsulatus* electron carriers with Fe-protein, we adopted an approach that has previously been developed and used for studying the interaction of NifF and Fe-protein with *K. pneumoniae* components [11]. It is

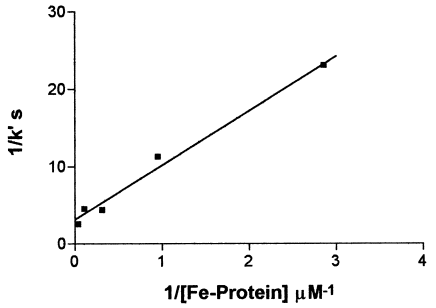

Fig. 6. Reduction of $NifF_{SQ}$ by dithionite catalyzed by Fe-protein. The data were obtained by stopped-flow spectrophotometry at 580 nm with: [$NifF_{SQ}$], 10.5 μM; dithionite, 0.85 mM; and Fe-protein varied between 0.35 and 28.4 μM. Data are plotted as $1/k'$ (where $k' = k_{obs} - k_{obs}$ ([Fe-P] = 0) versus 1/[Fe-protein].

not possible to measure the rates of electron transfer in the physiologically important direction [$NifF_{HQ}$ to Fe-protein] as this reaction is too fast to measure using conventional stopped-flow spectrophotometry (see also [11]). Therefore, we measured this reaction in the thermodynamically unfavourable direction, $(Fe\text{-protein})_{red}$ to $NifF_{SQ}$. In the presence of dithionite, the following reaction scheme (adapted from [11]) applies:

$$NifF_{SQ} + [Fe\text{-}P]_{red} \underset{k_{-1}}{\overset{k_{+1}}{\rightleftharpoons}} NifF_{SQ}[Fe\text{-}P]_{red} \underset{k_{-2}}{\overset{k_{+2}}{\rightleftharpoons}} NifF_{HQ}[Fe\text{-}P]_{OX} \underset{k_{-3}}{\overset{k_{+3}}{\rightleftharpoons}} NifF_{HQ} + [Fe\text{-}P]_{ox}$$

$$SO_3^{2+}\ k_{-4} \uparrow\downarrow k_{+4}\ SO_2^{\cdot-} \qquad\qquad SO_3^{-}\ k_{-5} \uparrow\downarrow k_{+5}\ SO_2^{\cdot-}$$

$$NifF_{HQ} \qquad\qquad [Fe\text{-}P]_{red}$$

Under these conditions, electron transfer between $[Fe\text{-}P]_{red}$ and $NifF_{SQ}$ can be directly observed by stopped-flow spectrophotometry due to the rapid removal of $[Fe\text{-}P]_{ox}$ by $SO_2^{\bullet-}$, k_{+5}, which effectively suppresses the back reactions, k_{-1}, k_{-2}, k_{-3}. In the experiments described here the change in absorbance at 580 nm (i.e. reduction of NifF) was well described by a single exponential and the amplitude change corresponded to complete reduction to the hydroquinone state, $k_{+3} \gg k_{+2}$. Therefore the rate of reduction of $NifF_{SQ}$ by Fe-protein can be described by:

If rapid pre-equilibrium binding of NifF to Fe-protein is assumed (i.e. $k_{-1} \gg k_{+2}$), then $(k_{+2}+k_{-1})/k_{+1}$ reduces to $k_{-1}/k_{+1} = K_d$, the dissociation constant for the complex. (Obviously an analogous treatment applies to interaction of FdI and Fe-protein.) Here, we have applied this analysis to the *R. capsulatus* system, i.e. we examined the interaction of NifF and FdI with the Fe-protein of nitrogenase by examining their reduction by Fe-protein in the presence of sodium dithionite. For the reduction of FdI, a plot of k', where $k' = k_{obs} - k_{obs}$ ([Fe-P] = 0), versus [Fe-protein] was linear (Fig. 5), indicating that the reaction was not saturated. The amplitude change observed was consistent with complete reduction of FdI. The slope therefore gives an apparent bimolecular rate $K_d k_{+2}$. A lower limit to K_d can be estimated as $K \geq 325$ μM (Table 2), if one assumes that curvature would have been observed at the highest [Fe-protein] if it was 20% of K_d. Thus FdI binds only weakly to reduced Fe-protein. On the other hand, the reduction of $NifF_{SQ}$ by reduced Fe-protein showed saturation, and the pre-equilibrium binding constant K_d could be directly determined from a plot of $1/k'$ versus 1/[Fe-protein] (Fig. 6). The determined K_d was 0.44 μM (Table 2), thus binding of NifF to Fe-protein is at least three orders of magnitude greater than the binding of FdI.

We examined the potential role of electrostatic interactions in the reaction between $NifF_{SQ}$ and reduced-Fe-protein by examining the variation in k_{obs} with ionic strength (varied by addition of NaCl up to a final concentration of 0.81 M). The linear portion of a plot of ln k_{obs} versus $[NaCl]^{1/2}$ gave a slope of -0.485 ± 0.084 (results not shown). Redox reactions in which electrostatic interactions have been shown

$$k_{obs} = k_{-4} K_{DT} [S_2O_4^{2-}]^{1/2} [NifF_{SQ}] + \frac{k_{+2}\,[Fe\text{-}P]_{red}\,[NifF_{SQ}]}{\frac{k_{+2}+k_{-1}}{k_{+1}} + [Fe\text{-}P]_{red}}$$

Table 2
Bimolecular rate constants determined by stopped-flow spectrophotometry

Reactants	k_2	K_d
FdII ($[S_2O_4]$)	16.5 ± 1.05 $M^{-1/2}$ s^{-1}	
FdI ($[S_2O_4]$)	1.69 ± 0.14 $M^{-1/2}$ s^{-1}	
NifF(HQ) ([FdI])	$2.08 \pm 0.05 \times 10^3$ M^{-1} s^{-1}	≥850 μM
NifF(HQ) ([FdII])	$24 \pm 1 \times 10^3$ M^{-1} s^{-1}	≥188 μM
NifF(SQ) ([FdI])	$12.5 \pm 1.2 \times 10^3$ M^{-1} s^{-1}	≥2500 μM
FdI_{OX} ([Fe-Protein]+DT)	$7.79 \pm 1.1 \times 10^2$ M^{-1} s^{-1}	≥325 μM
$NifF_{SQ}$ ([Fe-Protein]+DT)	7.05×10^6 M^{-1} s^{-1}	0.44 μM

to be important demonstrate a much more marked dependence of the second-order rate constant on ionic strength. For example, ln k_2 versus $I^{1/2}$ for the oxidation of flavodoxin semiquinone by cytochrome *c* has a gradient of −26 [4] and this measure for the reduction of cytochrome *c* by flavocytochrome b_2 is −5.9 [38]. Thus, electrostatic forces, either positive or negative, do not play a significant role in the interaction of NifF and Fe-protein. Ionic interactions have previously been shown to be important in the interaction of Fe-protein and Mo-Fe-protein [39,40]. This is the first demonstration that the tight complex observed between NifF and Fe-protein ([11], this study) is not primarily due to ionic interactions between the two redox partners.

4. Conclusion

In this study we have carried out an initial kinetic characterisation, using components derived from *R. capsulatus*, of the interaction of FdI and NifF and these proteins with the Fe-protein of nitrogenase. We observed tight-binding between NifF and Fe-protein, but not between FdI and Fe-protein. In a previous equilibrium kinetic study where the amount of FdI added to a coupled system consisting of chloroplast fragments and nitrogenase was varied, an apparent K_m of ∼1 μM was determined [33]. However, in this type of analysis, it is not possible to infer a disassociation constant for FdI and nitrogenase since the reaction involves multiple steps and clearly is not described by a simple Michaelis–Menton mechanism. Thus it is not clear what relationship this apparent K_m has with K_d. In the present study, transient kinetic analysis, which offers a method for the direct determination of dissociation constants, was used to determine K_d, for FdI, NifF, and the Fe-protein component of nitrogenase. In the only other transient kinetic study of the interaction of electron carriers with nitrogenase [11], tight binding was observed between NifF and Fe-protein from *K. pneumoniae*, but in that case tight complex formation required that the Fe-protein was complexed with MgATP or MgADP. Thus we have extended the previous studies to another bacterial system. Further studies are needed to determine the effect of the presence of MgATP or MgADP on the *R. capsulatus* system.

It would be interesting to attempt to extrapolate our results to the in vivo reduction of nitrogenase; however, at present only rough estimates of the in vivo concentrations the relevant redox proteins can be made. Based upon purification results [14,26,23] and immunoblot analysis [24], the approximate levels of these proteins are: Fe-protein, 25 μM; FdI, 54 μM; NifF, 3.9 μM, giving a molar ratio of 1:2.2:0.16. The results reported here indicate that FdI, although present in high levels in vivo, interacts only poorly in vitro with Fe-protein. It has been previously suggested that in some organisms with multiple low potential electron carriers, ferredoxin and flavodoxin form a sequential electron transfer chain to nitrogenase [12]. This appears to be unlikely for *R. capsulatus* since we were unable to find any evidence for specific complex formation between FdI and NifF. These considerations along with the approximate molar ratio of these proteins and the midpoint potentials and kinetic constants determined here, suggest that: (1) nitrogenase reduction by NifF is significant even though NifF is present in much smaller quantities that FdI; (2) NifF probably does not function as a redox mediator between FdI and Fe-protein, but may form a parallel electron

path to nitrogenase, or interact with its own specific reductase; and (3) the ultimate reductant should have an $E_m > -500$ mV and Fe-protein an E_m of ~ -440 mV, intermediate between that of *K. pneumoniae* (-398 mV) and *A. vinelandii* (-480 mV).

Acknowledgements

This work was supported in part by Grant OGP0036584 from the Natural Sciences and Engineering Research Council of Canada (to P.C.H.), The sabbatical stay of P.C.H. in the laboratory of Dr. Roger Thorneley was supported by a Bourse de Perfectionnement pour Chercheur Autonome (941776) from the Fonds de la Recherche en Santé du Québec, and by the Royal Society of the United Kingdom. Dr. Roger Thorneley is gratefully acknowledged for initiating us to stopped-flow methodology and for the use of his anaerobic stopped-flow spectrophotometer.

References

[1] S.G. Mayhew, H. Tollin, in: F. Muller (Ed.), Chemistry and Biochemistry of Flavoenzymes, Vol. III, CRC Press, Boca Raton, FL, 1992, pp. 389–426.
[2] C.T. Przysiecki, G. Cheddar, T.E. Meyer, G. Tollin, M.A. Cusanovich, Biochemistry 24 (1985) 5647–5652.
[3] J. Jung, G. Tollin, Biochemistry 20 (1981) 5124–5131.
[4] R.P. Simondsen, G. Tollin, Biochemistry 22 (1983) 3008–3016.
[5] R.P. Simondsen, P.C. Weber, F.R. Salemme, G. Tollin, Biochemistry 21 (1982) 6366–6375.
[6] P.C. Weber, G. Tollin, J. Biol. Chem. 260 (1985) 5568–5573.
[7] G. Tollin, G. Cheddar, J.A. Watkins, T.E. Meyer, M.A. Cusanovich, Biochemistry 23 (1984) 6345–6349.
[8] R.D. De Francesco, D.E. Edmondson, I. Moura, J.J.G. Moura, J. LeGall, Biochemistry 33 (1994) 10386–10392.
[9] T.E. Meyer, G. Cheddar, R.G. Bartsch, E.D. Getzoff, M.A. Cusanovich, G. Tollin, Biochemistry 25 (1986) 1383–1390.
[10] G. Cheddar, T.E. Meyer, M.A. Cusanovich, C.D. Stout, G. Tollin, Biochemistry 25 (1986) 6502–6507.
[11] R.N.F. Thorneley, J. Deistung, Biochem. J. 253 (1988) 587–595.
[12] J.R. Benemann, D.C. Yoch, R.C. Valentine, D.I. Arnon, Biochim. Biophys. Acta 226 (1971) 205–212.
[13] A.E. Martin, B.K. Burgess, S.E. Iismaa, C.T. Smartt, M.R. Jacobson, D.R. Dean, J. Bacteriol. 171 (1989) 3162–3167.
[14] P.C. Hallenbeck, Y. Jouanneau, P.M. Vignais, Biochim. Biophys. Acta 681 (1982) 168–176.
[15] A.F. Yakunin, I.N. Gogotov, Biochim. Biophys. Acta 725 (1983) 298–308.
[16] E. Schatt, Y. Jouanneau, P.M. Vignais, J. Bacteriol. 171 (1989) 6218–6226.
[17] K. Saeki, Y. Suetsugu, Y. Yao, T. Horio, B.L. Marrs, H. Matsubara, J. Biochem. 108 (1990) 474–482.
[18] C. Moreno-Vivian, S. Hennecke, A. Pühler, W. Klipp, J. Bacteriol. 171 (1989) 2591–2598.
[19] Y. Jouanneau, C. Meyer, J. Gaillard, E. Forest, J. Gagnon, J. Biol. Chem. 268 (1993) 10636–10644.
[20] I. Naud, M. Vincon, J. Garin, J. Gaillard, E. Forest, Y. Jouanneau, Eur. J. Biochem. 222 (1994) 933–939.
[21] C. Grabau, E. Schatt, Y. Jouanneau, P.M. Vignais, J. Biol. Chem. 266 (1991) 3294–3299.
[22] J. Armengaud, C. Meyer, Y. Jouanneau, Biochem. J. 300 (1994) 413–418.
[23] A.F. Yakunin, G. Gennaro, P.C. Hallenbeck, J. Bacteriol. 175 (1993) 6775–6780.
[24] G. Gennaro, P. Hübner, U. Sandmeier, A.F. Yakunin, P.C. Hallenbeck, J. Bacteriol. 178 (1996) 3949–3952.
[25] Y. Jouanneau, C. Meyer, I. Naud, W. Klipp, Biochim. Biophys. Acta 1232 (1995) 33–42.
[26] P.C. Hallenbeck, C. Meyer, P.M. Vignais, J. Bacteriol. 142 (1982) 708–717.
[27] M.A. Innis, D.H. Gelfand, J.J. Sninsky, T.J. White, PCR Protocols: A Guide to Methods and Applications, Academic Press, 1990.
[28] Y. Ichichara, Y. Kurosawa, Gene 130 (1993) 153–154.
[29] E.R. Zabarovsky, G. Winberg, Nucleic Acids Res. 18 (1990) 5912.
[30] R.N.F. Thorneley, C. Abell, G.A. Ashby, M.H. Drummond, R.R. Eady, S. Huff, C.J. Macdonald, A. Shneier, Biochemistry 31 (1992) 1216–1224.
[31] J. Deistung, R.N.F. Thorneley, Biochem. J. 239 (1986) 69–75.
[32] K. Saeki, K. Tokuda, K. Fukuyama, H. Matsubara, K. Nadanami, M. Go, I. Shigeru, J. Biol. Chem. 271 (1996) 31399–31406.
[33] I. Naud, C. Meyer, L. David, J. Breton, J. Gaillard, Y. Jouanneau, Eur. J. Biochem. 237 (1996) 399–405.
[34] J. Armengaud, J. Gaillard, E. Forest, Y. Jouanneau, Eur. J. Biochem. 231 (1995) 396–404.
[35] D.O. Lambeth, G. Palmer, J. Biol. Chem. 248 (1973) 6095–6103.
[36] R.N.F. Thorneley, D. Lowe, Biochem. J. 215 (1983) 393–403.
[37] C. Capeillère-Blandin, F. Guerlesquin, M. Bruschi, Biochim. Biophys. Acta 848 (1986) 279–293.
[38] S. Daff, R.E. Sharp, D.M. Short, C. Bell, P. White, F.D.C. Manson, G.A. Reid, S.K. Chapman, Biochemistry 35 (1996) 6351–6357.
[39] J. Kim, D.C. Rees, Nature 360 (1992) 553–560.
[40] H. Schindelin, C. Kisker, J.L. Schlessman, J.B. Howard, D.C. Rees, Nature 387 (1997) 370–376.